# Satellite-Based Pollution Monitoring in Prince William Sound – Deliverable 3: Final Report

**Report**
**R-15-049-1238**

**Prepared for:**
**Prince William Sound Regional Citizens' Advisory Council**

**Revision 1.1**
**January, 2016**

Captain Robert A. Bartlett Building
Morrissey Road
St. John's, NL
Canada A1B 3X5

T: (709) 864-8354
F: (709) 864-4706

Info@c-core.ca
www.c-core.ca

Registered to ISO 9001:2008

*This page is intentionally left blank*

# Satellite-Based Pollution Monitoring in Prince William Sound – Deliverable 3: Final Report

**Prepared for:**

Prince William Sound Regional Citizens' Advisory Council

**Prepared by:**

C-CORE

**C-CORE Report Number:**

R-15-049-1238
Revision 1.1
January, 2016


Smart Solutions for Challenging Environments

Captain Robert A. Bartlett Building
Morrissey Road
St. John's, NL
Canada A1B 3X5

T: (709) 864-8354
F: (709) 864-4706

Info@c-core.ca
www.c-core.ca



Registered to ISO 9001:2008

**The correct citation for this report is:**
C-CORE. (2016). *Satellite-Based Pollution Monitoring in Prince William Sound – Deliverable 3: Final Report*, C-CORE Report R-15-049-1238, Revision 1.1.

**Project Team**

Thomas Puestow (Project Manager)
Andrew Cuff
Sherry Warren

## REVISION HISTORY

| VERSION | SVN | NAME | COMPANY | DATE OF CHANGES | COMMENTS |
|---|---|---|---|---|---|
| 1.0 | 83 | Thomas Puestow | C-CORE | 25/11/2015 | Submitted to Client |
| 1.1 | 84 | Thomas Puestow | C-CORE | 08/01/2016 | Submission of Revised Version |
| | | | | | |
| | | | | | |
| | | | | | |

## DISTRIBUTION LIST

| COMPANY | NAME | NUMBER OF COPIES |
|---|---|---|
| Prince William Sound Regional Citizens' Advisory Council | Donna Schantz<br>Joseph Banta<br>Shawna Popovici | 1 electronic |
| | | |
| | | |

# TABLE OF CONTENTS

## LIST OF TABLES



## LIST OF FIGURES

# 1 INTRODUCTION

Prince William Sound (PWS) on the southern coast of Alaska is characterized by high volumes of marine traffic both commercial (oil tankers, fishing vessels) and recreational. The ability to detect potential pollution events is vital for the area's environmental and economic integrity. The Regional Citizens' Advisory Council (RCAC) was formed to promote environmentally safe pipeline and tanker operations throughout PWS and its adjacent waters. In an effort to support RCAC's mandate, this project was carried out to demonstrate the utility of satellite surveillance for environmental monitoring in PWS. Using freely available radar imagery from the recently launched Sentinel-1 mission, emphasis was placed on detecting potential oil slicks as well as large vessels transitioning PWS on their way to and from the Port of Valdez.

## 1.1 DOCUMENT STRUCTURE

Section 2 provides an overview of satellite-based oil spill monitoring technologies using synthetic aperture radar (SAR) sensors. The adopted approach, including data sources and processing methodology is presented in Section 3. Section 4 describes the results obtained and provides a discussion within the context of this study. Recommendations for future work are presented in Section 5. Applicable bibliographical references are presented in Section 6.

## 1.2 LIST OF ACRONYMS

| | |
|---|---|
| AOI | Area of Interest |
| AOOS | Alaska Ocean Observing System |
| CIS | Canadian Ice Service |
| EMSA | European Maritime Safety Agency |
| ESA | European Space Agency |
| GRD | Ground Range Detected |
| HR | High Resolution |
| ISTOP | Integrated Satellite Tracking of Pollution |
| IW | Sentinel-1 Interferometric Wideswath |
| NAD83 | North American Datum of 1983 |
| NOAA | National Oceanic and Atmospheric Administration |
| NSIDC | National Snow and Ice Data Center |
| PWS | Prince William Sound |
| QC | Quality Control |
| RCAC | Regional Citizens' Advisory Council |
| SAR | Synthetic Aperture Radar |
| SDH | Sentinel Scientific Data Hub |
| SLAR | Side-Looking Airborne Radar |
| UAV | Unmanned aerial vehicle |
| UTC | Coordinated Universal Time |
| UTM | Universal Transverse Mercator |

# 2 OIL SPILL MONITORING USING SATELLITE RADAR IMAGERY

Radar systems operate in the microwave spectrum, are largely weather-independent, can acquire images day and night and are available on airborne and satellite platforms. Radar backscatter signal depends on the parameters of the imaged surface such as target material, conductivity and system characteristics, such as wavelength, incidence angle and polarization (Campbell and Wynne, 2011). Radars use an antenna to emit and collect the microwave signal and spatial resolution improves as the length of the antenna increases (Van Zyl and Kim, 2011).

Due to the large antenna size, side-looking airborne radar (SLAR) is restricted to aerial platforms, typically fixed-wing planes. SAR by contrast, uses the forward motion of the sensor platform, while taking into account Doppler shift of the collected signal to synthetically increase antenna aperture (Gade et al., 1996). Imaging satellite radars rely on SAR, although airborne SAR sensors are also used. SAR satellite sensors have emerged as the predominant means of ice surveillance over large areas and are widely used by national ice centers around the world.

Oil slicks on water are detectable by radar imagery because of the dampened capillary waves which correspondingly reduces backscatter compared with the surrounding oil-free water (Solberg et al., 1999). Oil on water appears as dark patches on radar images (Topouzelis, 2008). Capillary waves are also reduced by other phenomena (e.g. natural surfactants, algal blooms) and verification by other means is required to identify oil unambiguously.

Most current radars operate in C-Band (wavelength ~5 cm) or X-Band (wavelength ~3 cm), although L-band (15 to 30 cm) and P-Band (30 to 100 cm) systems have been used on airborne and satellite platforms. Radars can be configured to transmit and receive horizontally or vertically polarized[1] radiation and vertical antenna polarizations for both transmission and reception (VV) have been shown to yield better results than other configurations for oil detection (Brekke and Solberg, 2005).

Wind speed is a major factor in detection of oil with radar. At low wind speeds, there is relatively little wave activity and almost no scattering from the ocean surface, minimizing the contrast between oil-affected and oil-free areas (Solberg et al., 1999). On the other hand, at very high wind speeds the larger waves are substantial enough to overcome damping effects caused by the oil. Again, under these conditions the brightness and contrast between the oil and surrounding water is diminished, and the presence of oil cannot be detected. In general, wind conditions between approximately 3 and 10 $ms^{-1}$ are favorable for detecting oil on open water using SLAR or SAR sensors (Gade et al., 1996; Solberg et al., 1999; Brekke and Solberg, 2005; Babiker et. al., 2010).

False alarms are possible from areas of low wind, biogenic slicks, fresh water inclusions, grease ice, shear zones and internal waves, all of which may have a radar signature similar to oil on water (e.g., Fingas and Brown, 1997; Solberg, 2012). Discriminating oil from the water background typically relies on analysis of local image contrast as well as shape and distribution of observed dark patches (Brekke and Solberg, 2005; Topouzelis, 2008).

[1] The polarization refers to the orientation of the antennas and, therefore, the radiated energy.

In the last decade, satellite-based oil spill monitoring has become an integral part of national pollution control programs in Europe and Canada (Ferraro et al., 2010). In Europe, the European Maritime Safety Agency (EMSA) administers satellite-based monitoring through a network of service providers, while in Canada the Integrated Surveillance and Tracking of Pollution (ISTOP) program is executed through the Canadian Ice Service (CIS). Figure 1 shows an example of a satellite SAR image with oil and ship signatures acquired and analyzed by CIS.

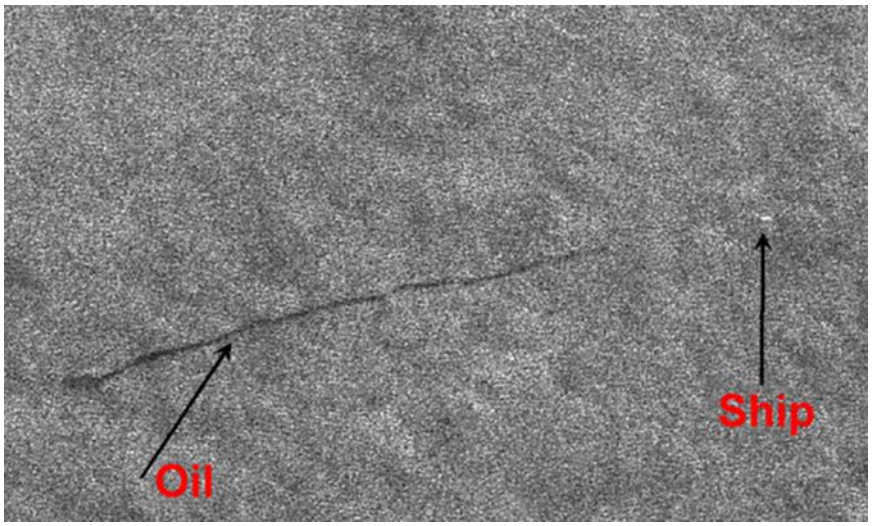


Figure 1. Satellite SAR image with oil and ship signatures (source: http://www.ec.gc.ca/glaces-ice/default.asp?lang=En&n=C5EE0C9F-1)

The approaches and algorithms used to extract potential oil slicks are typically divided into two major stages. In the first stage, areas of low backscatter are identified in the image either through manual interpretation or automated segmentation. In the second stage the characteristics of the low-backscatter areas are evaluated to determine if it is likely an oil slick. Classes of features used in this context are slick geometry and structure, appearance of the edges, brightness contrast to surrounding areas, known sea state, known presence of algae blooms and locations of ships or platforms (Brekke and Solberg, 2005; Solberg, et al., 2007; ASL, 2012).

The presence of oil slick look-alikes remains a constant issue, with false alarm rates ranging from 15 to 85% (Tarchi, 2005), however, recent research indicates that automated algorithms are increasingly able to differentiate between oil slicks and look-alikes, with classification accuracies ranging from 73% to 92% (Brekke and Solberg, 2005; Bogdanov et al., 2005; ASL, 2012). Present operational oil spill monitoring using satellite SAR is based on manual or semi-automatic interpretation with significant input from operators (Ferraro et al., 2010), suggesting that automated algorithms may not yet be able to fully take account of environmental conditions, look-alikes and slick characteristics encountered in the routine surveillance of large areas.

More recently, researchers have focused on examining the capability of fully-polarimetric SAR imagery to characterize oil slicks (Minchew et al., 2012; Solberg, 2012; ASL, 2012). In full polarimetry, a greater amount of information can be exploited as all horizontal and vertical components of the

electromagnetic radiation are supported for both transmission and reception at the sensor. As a result, a fully-polarimetric SAR image contains four image channels available for analysis as described in Table 1. The use of polarimetry for oil slick detection remains an active field of research and is not yet available for operational monitoring. An overview of current and future satellite SAR missions and supported polarizations is provided in Table 2.

Table 1. Current and future SAR satellites

| Polarization | Description |
|---|---|
| HH | Sensor transmits and receives horizontally polarized radiation |
| VV | Sensor transmits and receives vertically polarized radiation |
| HV | Sensor transmits horizontally polarized radiation and receives vertically polarized radiation |
| VH | Sensor transmits vertically polarized radiation and receives horizontally polarized radiation |

Table 2. Current and future SAR satellites

| Sensor | Band | Polarizations | Spatial Resolution [m] | Swath Width [km] | Revisit Frequency | Status |
|---|---|---|---|---|---|---|
| RADARSAT-1 | C | HH | 10 to 100 | 50 to 500 | 2 to 3 days | Safe Mode* |
| RADARSAT-2 | C | HH, VV, HV, VH | 1 to 100 | 50 to 500 | 2 to 3 days | Operational |
| COSMO-SKYMED | X | HH, VV, HV, VH | 1 to 100 | 10 to 200 | 2 days | Operational |
| TERRASAR-X | X | HH, VV, HH/VV, HH, HV, VV, VH | 1 to 18 | 10 to 150 | 3- 4 days | Operational |
| SENTINEL-1 | C | HH, VV, HH/VV, HH, HV, VV, VH | 20 | 250 | 1 to 3 days | Operational |
| RCM | C | HH, VV, HV, VH | 1 to 100 | 50 to 500 | Daily | Launch in 2018 |

* RADARSAT-1 stopped accepting new tasking requests in April 2013, but may become operational again

# 3 METHODOLOGY

This section describes the approach adopted for this investigation, including area of interest (AOI), satellite and ancillary data sources, as well as the analysis process flow.

## 3.1 AREA OF INTEREST

The general AOI for this investigation is presented by the yellow polygon in Figure 2. Wind-protected fjords and other sheltered areas within the AOI were excluded from the analysis if wind speed and backscatter information indicated an insufficient amount of surface roughness for detecting oil slicks. Efforts to detect vessels were concentrated on the shipping lane connecting the Port of Valdez to the Gulf of Alaska.

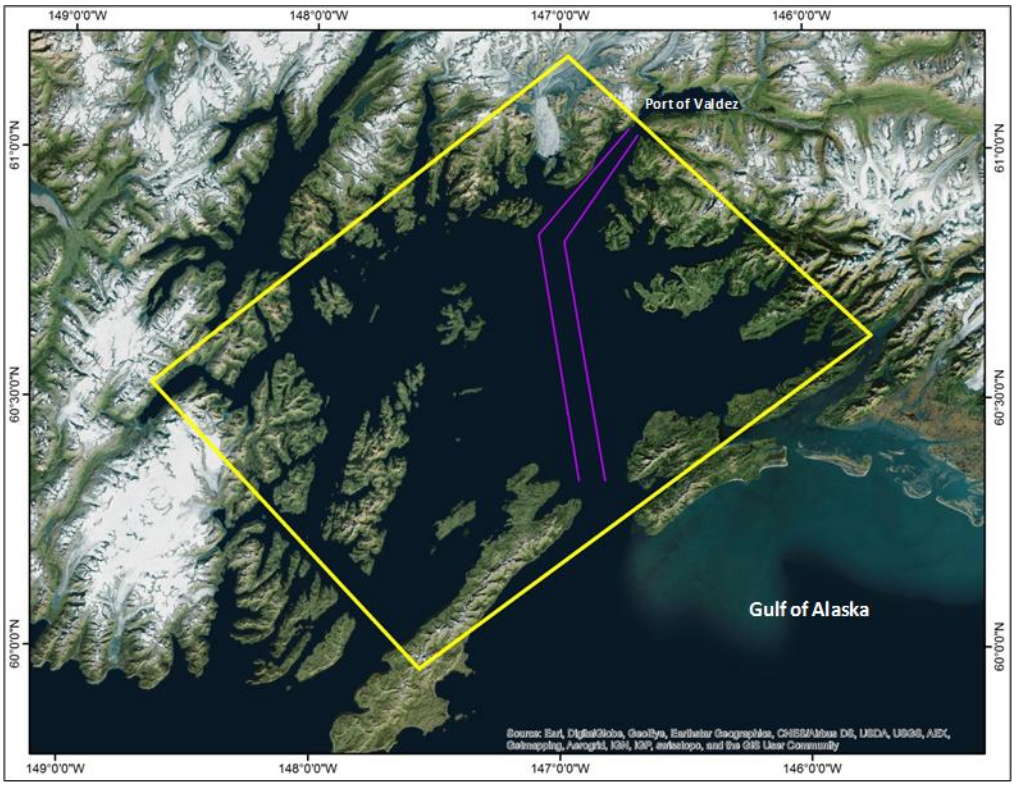


Figure 2. PWS AOI (yellow), shipping lane (purple)

## 3.2 SATELLITE DATA

The primary data source used for this investigation was Sentinel-1 Interferometric Wide Swath (IW) imagery. Launched in 2014, Sentinel-1 captures satellite SAR imagery systematically over designated areas without the need to plan acquisitions (ESA, 2015). Following a free and open data policy, Sentinel-1 imagery is freely available and can be accessed via European Space Agency's (ESA's) scientific data hub (SDH) (https://scihub.esa.int/). Table 3 presents characteristics of image data used in this study.

Table 3. Sentinel-1 sensor characteristics and IW parameters

| Parameter | Value |
|---|---|
| Frequency | C-band (5.405 GHz) |
| NESZ (noise floor) | -22 dB |
| Polarization | VV |
| Swath Width | 250 km |
| Radar Resolution | 20 m |
| Incidence Angle Range | $29^0$ - $46^0$ |
| Pixel Spacing | 10 m |
| Mode | IW |
| Product | Level-1 GRD, HR |

All images used in this study were processed to Level-1 ground range detected (GRD), high resolution (HR). GRD images contain focused SAR data that has been detected, multi-looked and projected to ground range using an earth ellipsoid model. With a nominal spatial resolution of 20 m, the resulting image product is resampled to a pixel spacing of 10 m (ESA, 2013). Figure 3 presents the various footprints of IW coverage available over the AOI.

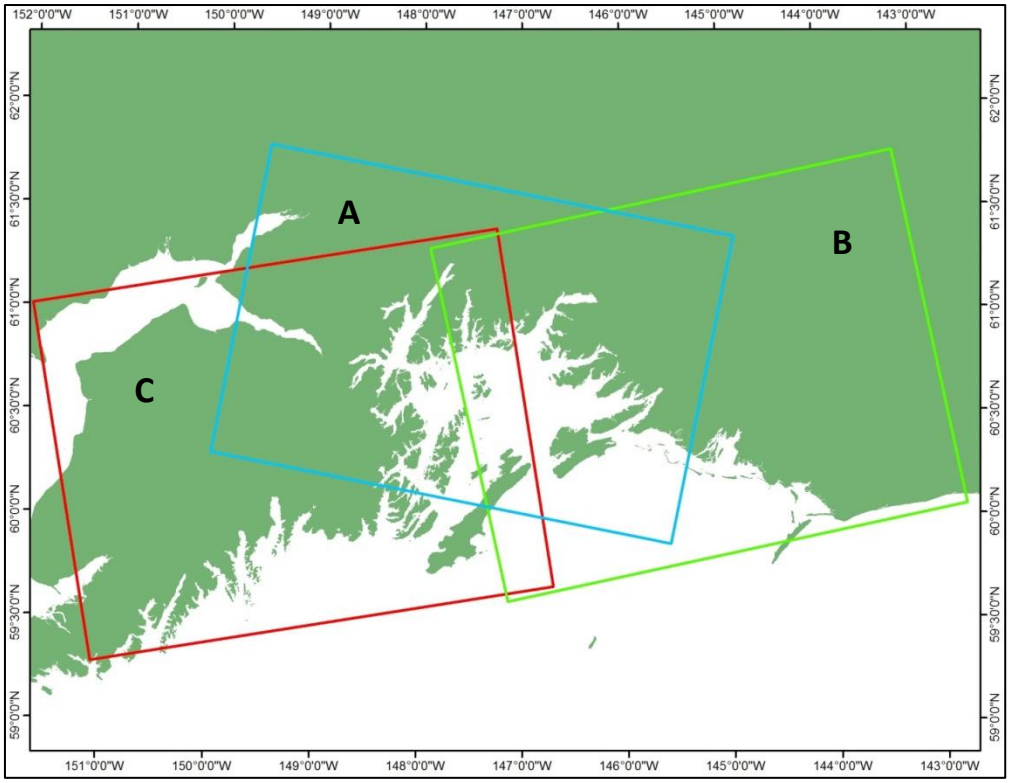


Figure 3. Footprint of Sentinel-1 IW passes over PWS

The AOI is fully covered by Area A (blue), while Areas B (green) and C (red) cover the eastern and western halves of PWS, respectively. According to the technical specifications of the Sentinel-1 mission, coverage of these areas is repeated every 12 days with a single satellite in orbit, and every 6 days with both satellites of the constellation in orbit (ESA, 2013). The acquisition of imagery alternates between ascending (i.e. satellite moves south to north) and descending (satellite moves north to south) passes.

Launched in April 2014, the Sentinel-1 mission is still ramping up towards a fully operational status. Accordingly, at the time of this investigation, only imagery acquired on descending orbits were available for Area A, whereas areas B and C were covered by imagery collected during ascending satellite passes. In addition, only 45% of the images expected to be acquired were actually available for retrieval from the SDH. Table 4 shows the resulting Sentinel-1 scenes used in this investigation. A total of 8 images acquired between June 1 and October 7, 2015, were analyzed.

Table 4. Sentinel-1 acquisitions over PWS

| Date [YYYY-MM-DD] | Time [UTC] | Orbit | Area Covered |
|---|---|---|---|
| 2015-06-01 | 16:12:36 | Descending | A |
| 2015-06-25 | 16:12:38 | Descending | A |
| 2015-07-03 | 03:19:26 | Ascending | B |
| 2015-07-19 | 16:12:38 | Descending | A |
| 2015-07-27 | 03:19:26 | Ascending | B |
| 2015-08-20 | 03:19:29 | Ascending | B |
| 2015-09-13 | 03:19:30 | Ascending | B |
| 2015-10-07 | 03:19:30 | Ascending | B |

According to ESA (2013), Sentinel-1 imagery should be available within 3 hours of acquisition. However, this standard has not yet been reached, and observed time lags between acquisition and posting to the SDH vary from less than three hours to several days. This situation is expected to improve in the near future. Once fully operational with two satellites acquiring data, the revisit frequency for any area covered will increase to 6 days (ESA, 2015).

## 3.3 ANCILLARY DATA

In addition to satellite imagery, a number of environmental observations were used to aid in image interpretation, including surface wind speed, the presence of sea ice, sea surface temperature, as well as algae blooms and the presence of aquatic vegetation. All ancillary datasets were accessed via the Alaska Ocean Observing System (AOOS) (http://www.aoos.org).

Within the context of SAR-based oil slick monitoring, wind speed at the time of image acquisition is of critical importance, with optimal conditions for slick detection for wind speeds ranging from 3 $ms^{-1}$ to 10 $ms^{-1}$. Fields of surface wind speed and direction at three-hour intervals were retrieved from AOOS. A summary of average, minimum and maximum wind speeds corresponding to each Sentinel-1 image is presented in Table 5.

Table 5. Summary of wind speed over AOI corresponding to each image acquisition

| Date [YYYY-MM-DD] | Time [UTC] | Average Wind Speed [$ms^{-1}$] | Maximum Wind Speed [$ms^{-1}$] | Minimum Wind Speed [$ms^{-1}$] |
|---|---|---|---|---|
| 2015-06-01 | 16:12:36 | 2.72 | 6.47 | 0.71 |
| 2015-06-25 | 16:12:38 | 4.52 | 7.86 | 0.86 |
| 2015-07-03 | 03:19:26 | 1.72 | 3.11 | 0.53 |
| 2015-07-19 | 16:12:38 | 2.25 | 3.57 | 0.95 |
| 2015-07-27 | 03:19:26 | 3.41 | 5.47 | 0.72 |
| 2015-08-20 | 03:19:29 | 1.23 | 3.26 | 0.30 |
| 2015-09-13 | 03:19:30 | 2.51 | 4.54 | 0.77 |
| 2015-10-07 | 03:19:30 | 3.04 | 5.89 | 0.76 |

Historical sea ice concentration data were reviewed to understand sea ice coverage in PWS. The National Snow and Ice Data Center (NSIDC) sea ice concentration dataset on the AOOS website provided information on sea ice concentrations through recent years. Based on this dataset sea ice usually only occurs in April and May and concentrations are typically less than 50%. While the data showed no sea ice in PWS in 2012, 2013 and 2014, sea ice was present in 2015 (see Figure 4). All images used in this investigation were acquired during ice-free conditions.

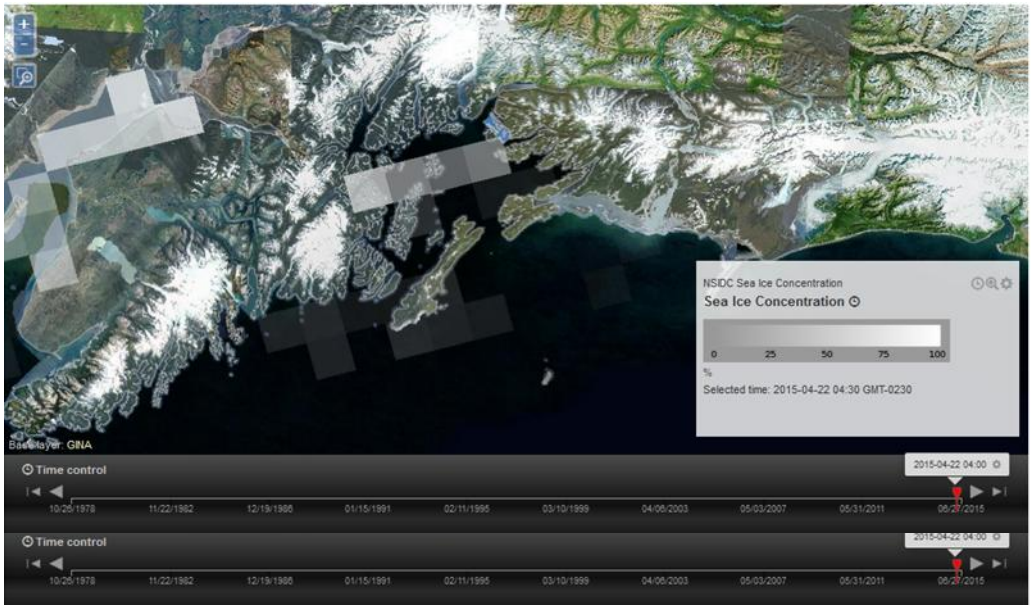


Figure 4. NSIDC sea ice concentration for April 22, 2015 in PWS (source: www.aoos.org)

Residual oil from the Exxon Valdez oil spill could exist in the area and cause false alarms for recent oil slick detection. However, the dataset on the AOOS website only shows residual oil from the spill for the shoreline and is therefore not applicable to open water applications.

## 3.4 IMAGE ANALYSIS

The focus of this investigation extended to both the detection of potential oil slicks and the detection of large vessels (e.g. tankers, container ships along the AOI's major shipping route). This was possible as the detection of slicks and vessels follow the same basic process flow as shown in Figure 5.

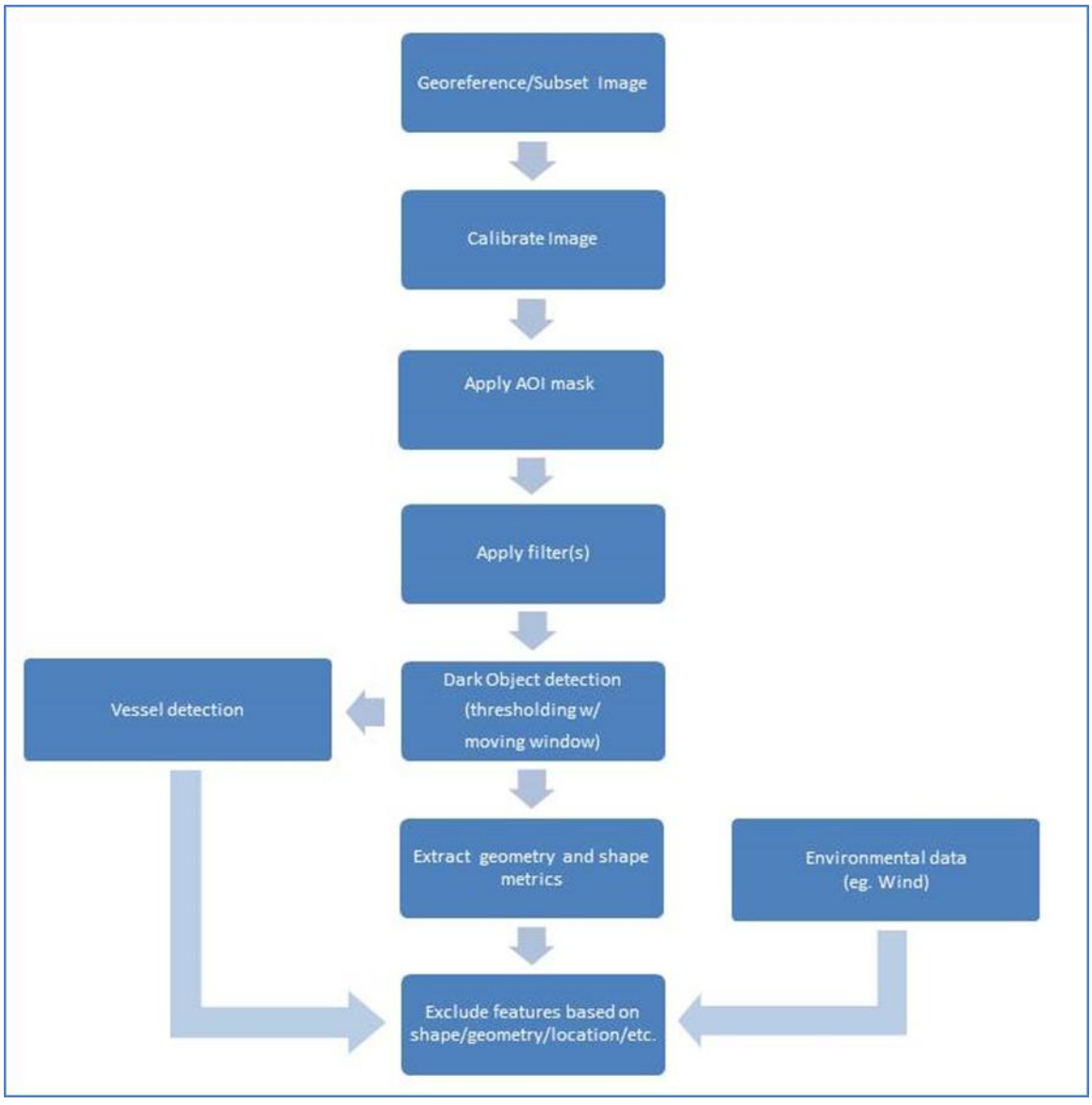


Figure 5. Process flow for analysis for vessel and slick detection

Sentinel-1 satellite images were retrieved from ESA's scientific data hub and subsequently processed using C-CORE's target detection software. All images were georeferenced to the Universal Transverse Mercator (UTM) coordinate system (Zone 6, North American Datum of 1983 (NAD83) and radiometrically calibrated to backscatter coefficient expressed as sigma naught. Land areas were

removed from the analysis by applying a land mask. The land mask was generated using shoreline vector data retrieved from the National Oceanic and Atmospheric Administration (NOAA) Shoreline Data Explorer website http://www.ngs.noaa.gov/NSDE/). The shoreline vectors were converted to polygon format, and a buffer of 500 meters was applied to remove small islands and shallow coastal areas from the analysis. Target detection requires the modeling of ocean backscatter using a K-distribution followed by adaptive thresholding to identify targets that are darker or brighter than their background. Examples of bright and dark target radar signatures are presented in Figure 6.

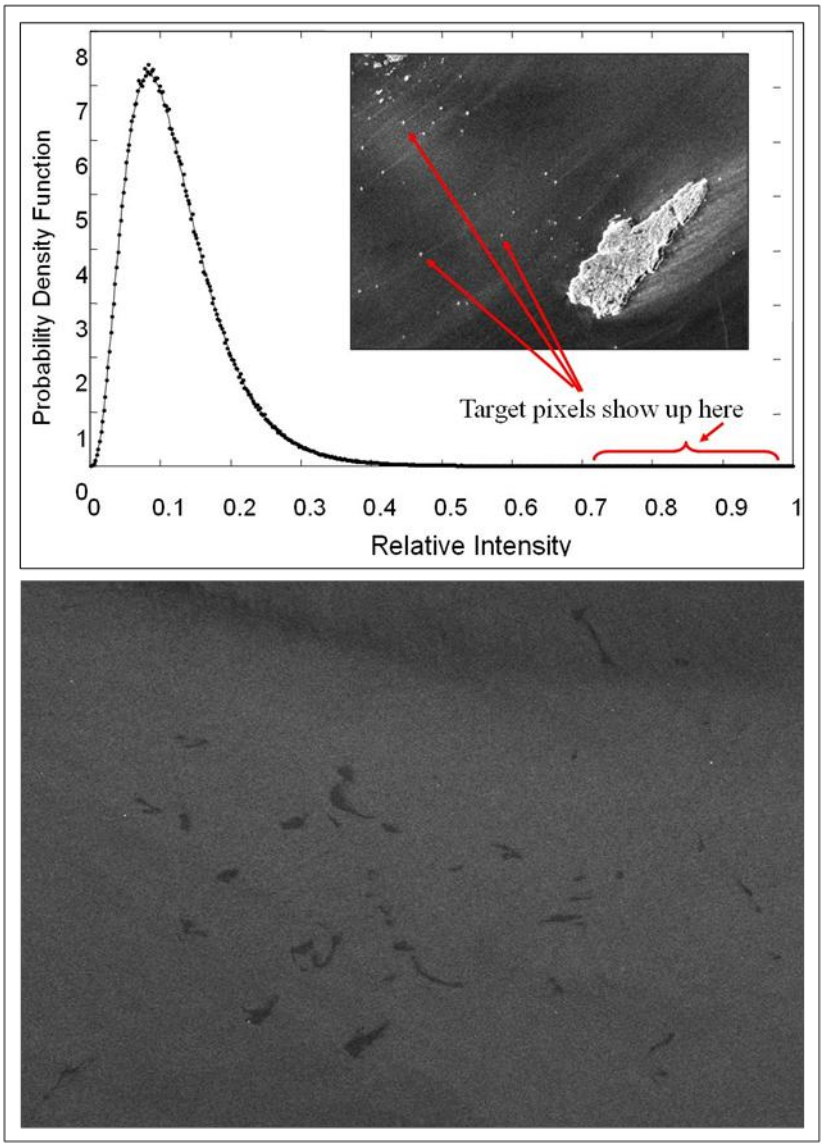


Figure 6. Example of bright and dark target pixels

Upon completion of the target detection process the image was visually assessed for potential oil slicks. The image analyst reviewed any dark areas, especially near detected vessels, and decided whether they were potential oil slicks based on their shape, geometry, location, ship locations, and wind conditions. At the final stage of the analysis an image analyst performed quality control (QC) on all detections to confirm whether they are valid targets.

# 4 RESULTS

Satellite monitoring of the AOI was carried out between June and October 2015, with a total of 8 monitoring products generated. The detection results for each image are presented in Table 6.

Table 6. Number of vessel and oil slick detections per image

| Date [YYYY-MM-DD] | Time [UTC] | Number of Oil Slicks Detected | Number of Vessels Detected |
|---|---|---|---|
| 2015-06-01 | 16:12:36 | 0 | 1 |
| 2015-06-25 | 16:12:38 | 0 | 3 |
| 2015-07-03 | 03:19:26 | 0 | 3 |
| 2015-07-19 | 16:12:38 | 0 | 1 |
| 2015-07-27 | 03:19:26 | 0 | 0 |
| 2015-08-20 | 03:19:29 | 0 | 0 |
| 2015-09-13 | 03:19:30 | 0 | 0 |
| 2015-10-07 | 03:19:30 | 0 | 3 |

Throughout the period of this demonstration, no potential oil slicks were detected. Slick-like radar signatures were prevalent in all images analyzed, but after close analysis these signature were determined to be likely caused by other factors, such as wind shadow, biogenic slicks, wakes of boats and ships, as well as convergent and divergent fronts separating water masses with different physical properties.

Monitoring the major shipping lane across the AOI returned 11 large vessel targets. Although not reported during this demonstration, nearly every image contained a much larger number of bright targets, which include smaller vessels as well as icebergs. However, these targets were not reported as the main focus of vessel detection was on large targets within the shipping lane. The monitoring products generated are presented in Figure 7 to Figure 14.

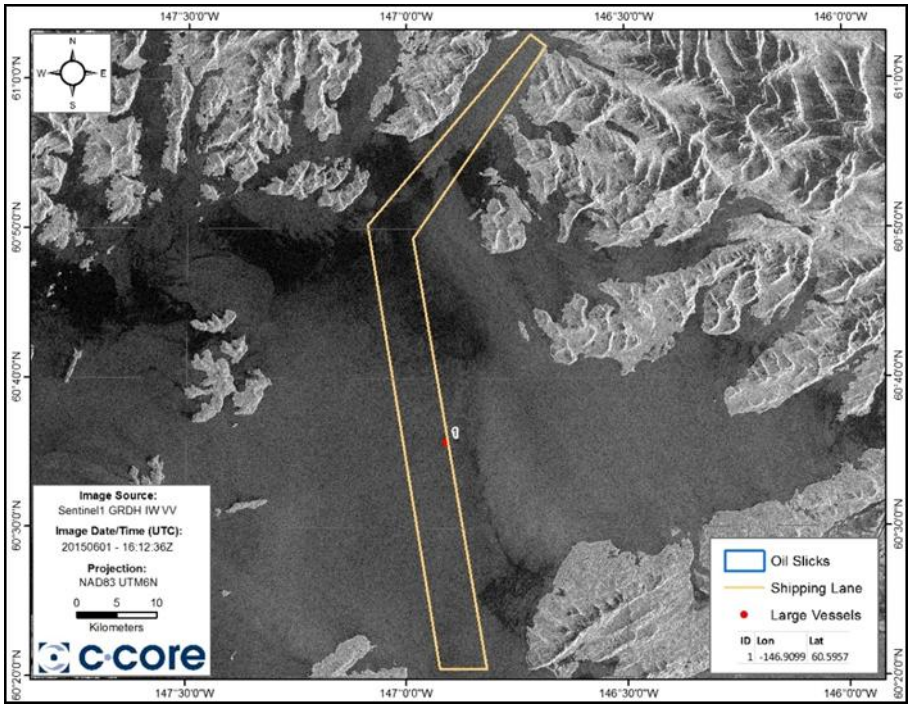


Figure 7. Monitoring product – June 1, 2015

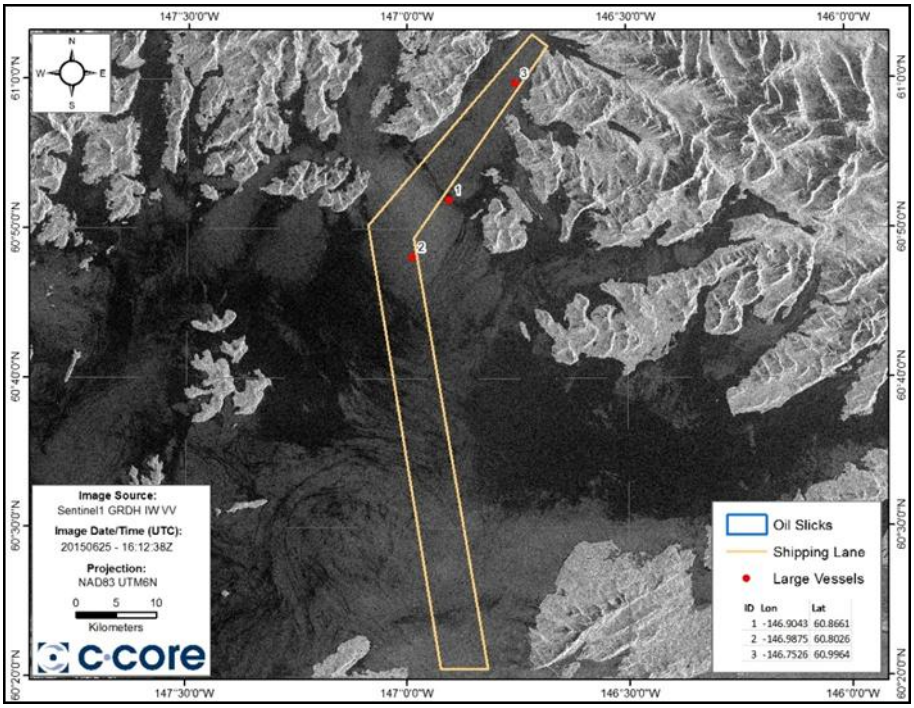


Figure 8. Monitoring product – June 25, 2015

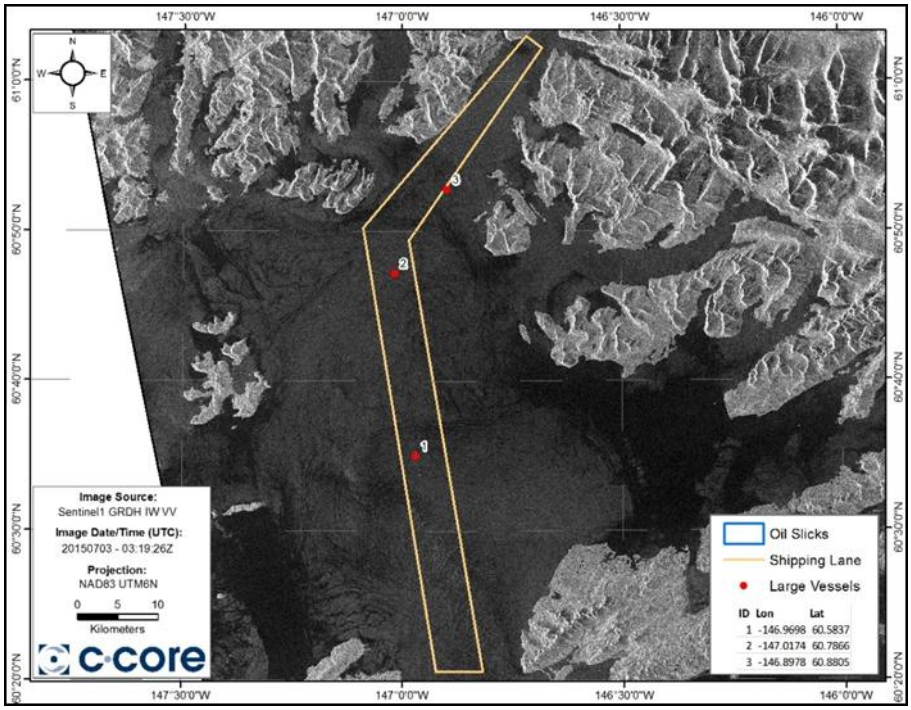


Figure 9. Monitoring product – July 3, 2015

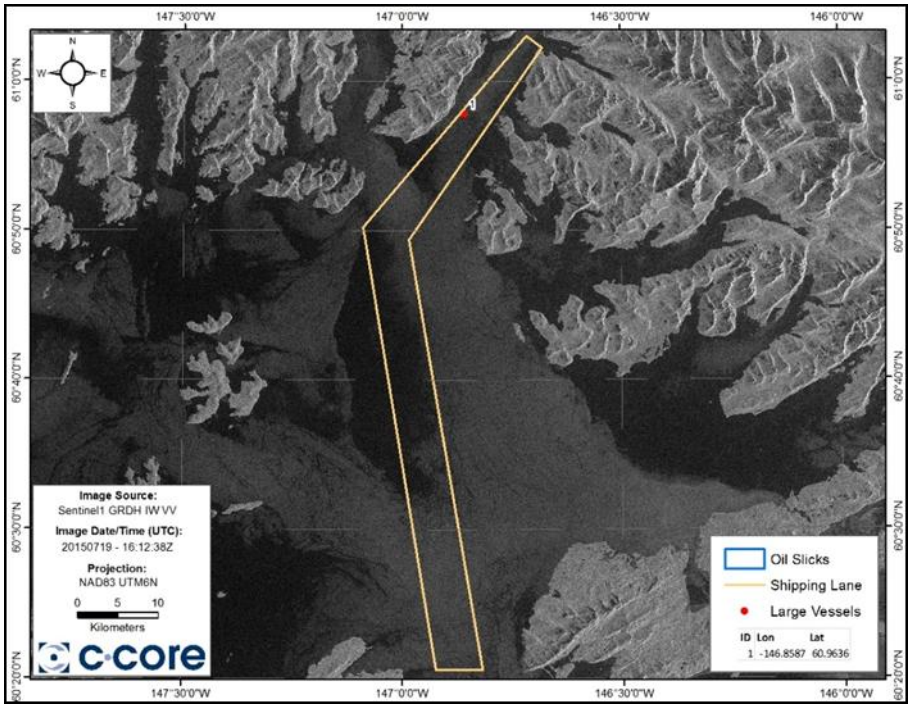


Figure 10. Monitoring product – July 19, 2015

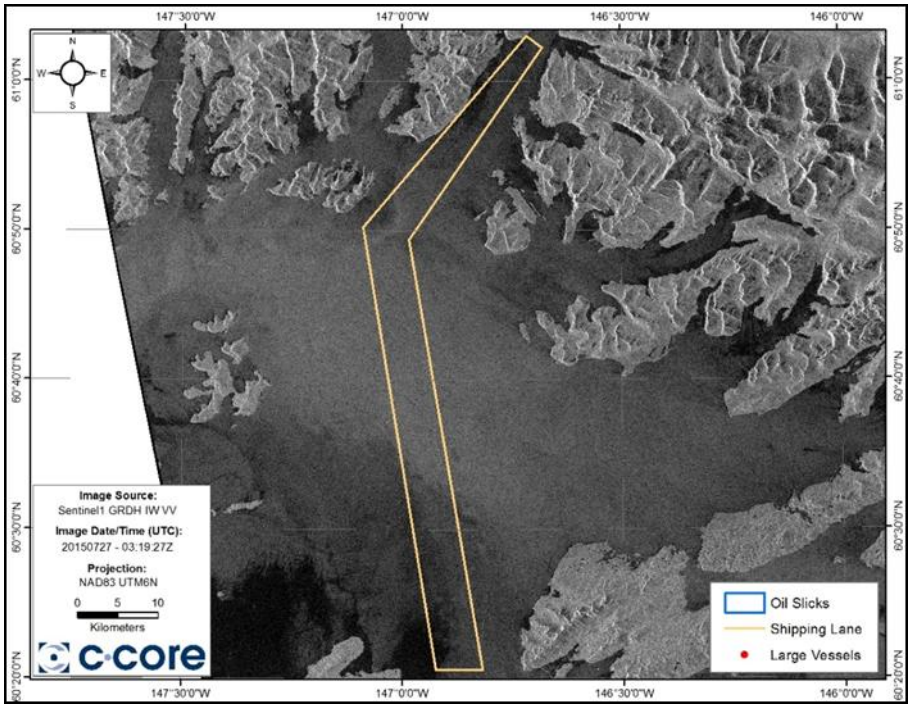


Figure 11. Monitoring product – July 27, 2015

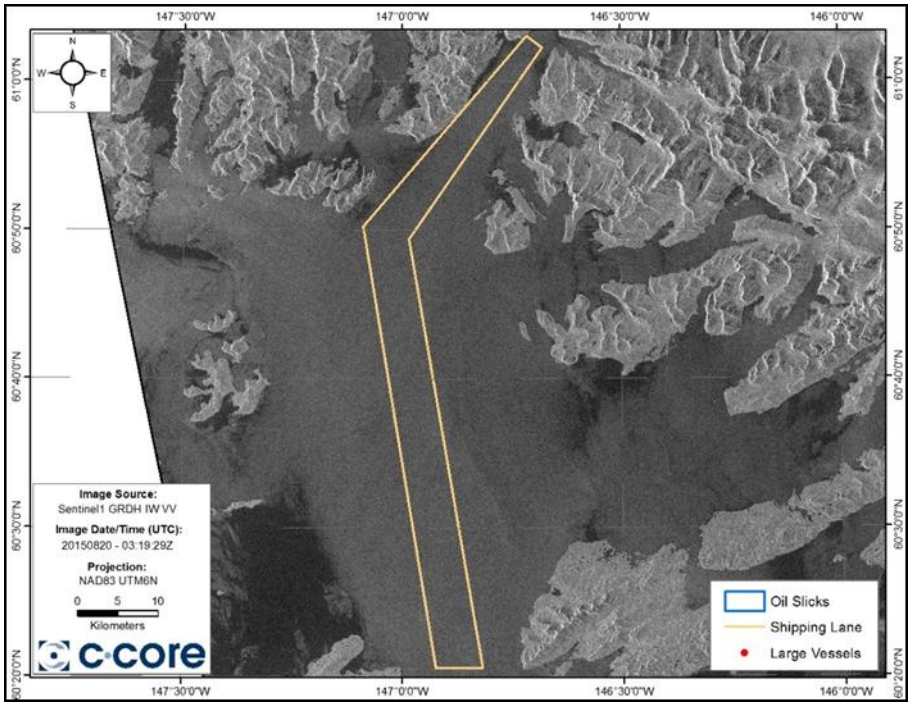


Figure 12. Monitoring product – August 20, 2015

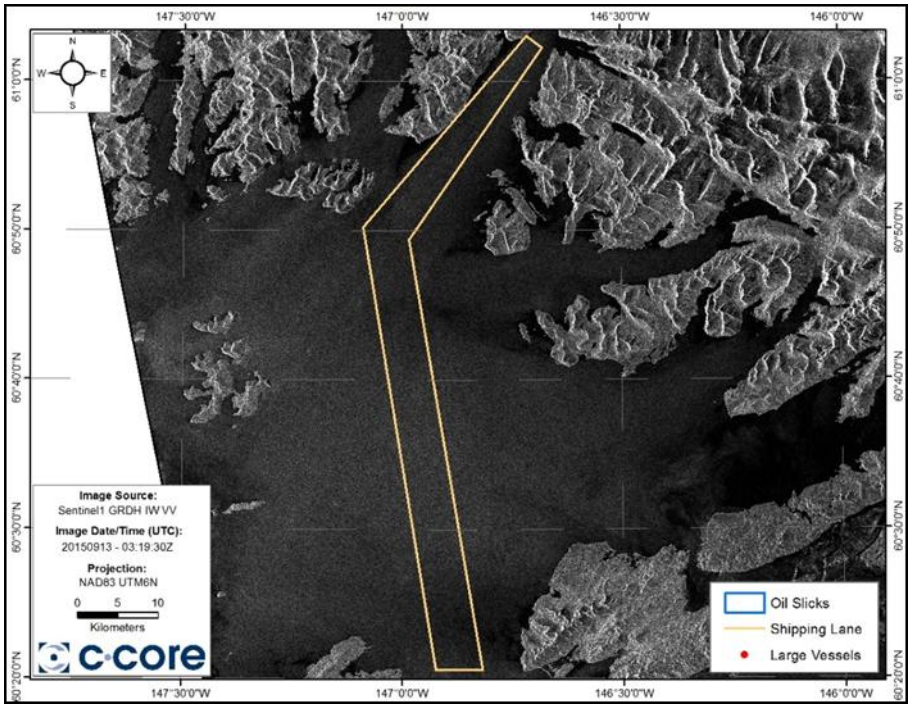


Figure 13. Monitoring product – September 13, 2015

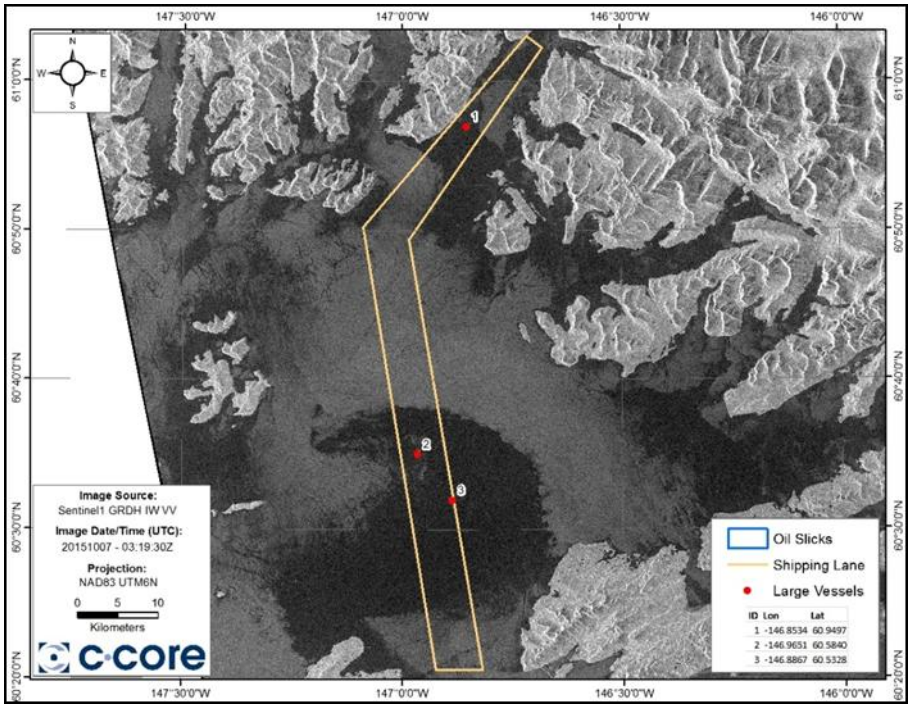


Figure 14. Monitoring product – October 7, 2015

# 5 DISCUSSION

Although maritime traffic and residual oil from previous spills constitute possible sources of oil slicks in PWS, no potential oil slicks were detected during this investigation. This is not surprising given the biophysical complexity of the AOI and a generally low probability of occurrence of voluntary or accidental oil spills. For example, Environment Canada's ISTOP program is relying on satellite radar imagery to survey Canadian waters for illegal discharge. Table 7 provides a summary of the number of satellite images analyzed together with the resulting potential oil slicks detected. With more than 10,000 satellite images processed since 2006, only 258 possible oil slicks were identified in Canadian waters. This corresponds to approximately 50 images processed on average to detect one potential slick. Table 7 also shows a steady decline of detected slicks over the same time frame.

Table 7. Summary of ISTOP surveillance results (Environment Canada, 2015)

| Fiscal Year | Number of Analyzed Images | Number Potential Oil Slicks Detected |
|---|---|---|
| 2006-2007 | 1,044 | 39 |
| 2007-2008 | 1,049 | 44 |
| 2008-2009 | 1,216 | 34 |
| 2009-2010 | 1,148 | 23 |
| 2010-2011 | 972 | 18 |
| 2011-2012 | 1076 | 22 |
| 2012-2013 | 1239 | 16 |
| 2013-2014 | 1104 | 12 |
| 2014-2015 | 2109 | 50 |

Europe's CleanSeaNet initiative relies on satellite imagery to monitor European waters for oil spills, with emphasis on the Mediterranean Sea, the Atlantic coast and the Baltic Sea. While ISTOP and CleanSeaNet process a comparable number of satellite images on a yearly basis, the number of detected potential slicks per image is much higher for CleanSeaNet. This is likely a reflection of the higher marine traffic density in European waters compared to Canada. Similarly to ISTOP, CleanSeaNet also shows a global reduction in the number of potential slicks detected per image from 1.38 in 2008 to 0.75 in 2009 (EMSA, 2011). The observed decline in detections under ISTOP and CleanSeaNet suggests that the current satellite monitoring programs in Canada and Europe are effective measures of deterrence. Particularly important in this context is the regular, public promotion of the surveillance program as a means of ensuring regulatory compliance.

The validation of satellite-based oil slick detections is challenging due to the need to visit the location of potential spill before the oil dissipates. This typically requires field verification by aircraft or vessel within 2 to 3 hours of the satellite overpass. Effective validation therefore depends on a variety of factors such as number and location of available resources and assets (i.e. aircraft and vessels), distance of potential spill from assets and suitable environmental conditions.

Both ISTOP and CleanSeaNet are designed to provide surveillance over large areas and identify instances of potential pollution that should be confirmed by field verification (usually via aircraft). To this end, the satellite detection products are assigned different levels of priority to allow the most effective use of resources for field verification. ISTOP assigns priority based on different elements of the slick's signature, such as contrast, edges and, shape, together with the potential source, surrounding ocean surface characteristics, as well as wind speed and direction (Ferraro et al., 2010). CleanSeaNet defines alert levels based on the likelihood of the reported spill being oil, the probability that a polluter can be identified and the level of potential damage to the environment caused by an oil spill (EMSA, 2015). Approximately 32% of all CleanSeaNet satellite detections were selected for further verification in the field. Between 2009 and 2011, 50% of satellite detections verified by aerial surveillance were confirmed to be pollutant spills.

The technology underlying ISTOP, CleanSeaNet and similar programs has been developed since the early 1990s. Accordingly, satellite-based oil slick monitoring is considered fully operational and applicable anywhere in the world within the limitations inherent in the technology as described in Section 2. Figure 15 and Figure 16 show example detection products generated by ISTOP and CleanSeaNet, respectively. Figure 15 shows an oil slick off the coast of Newfoundland (yellow), nearby ship positions are marked in blue.

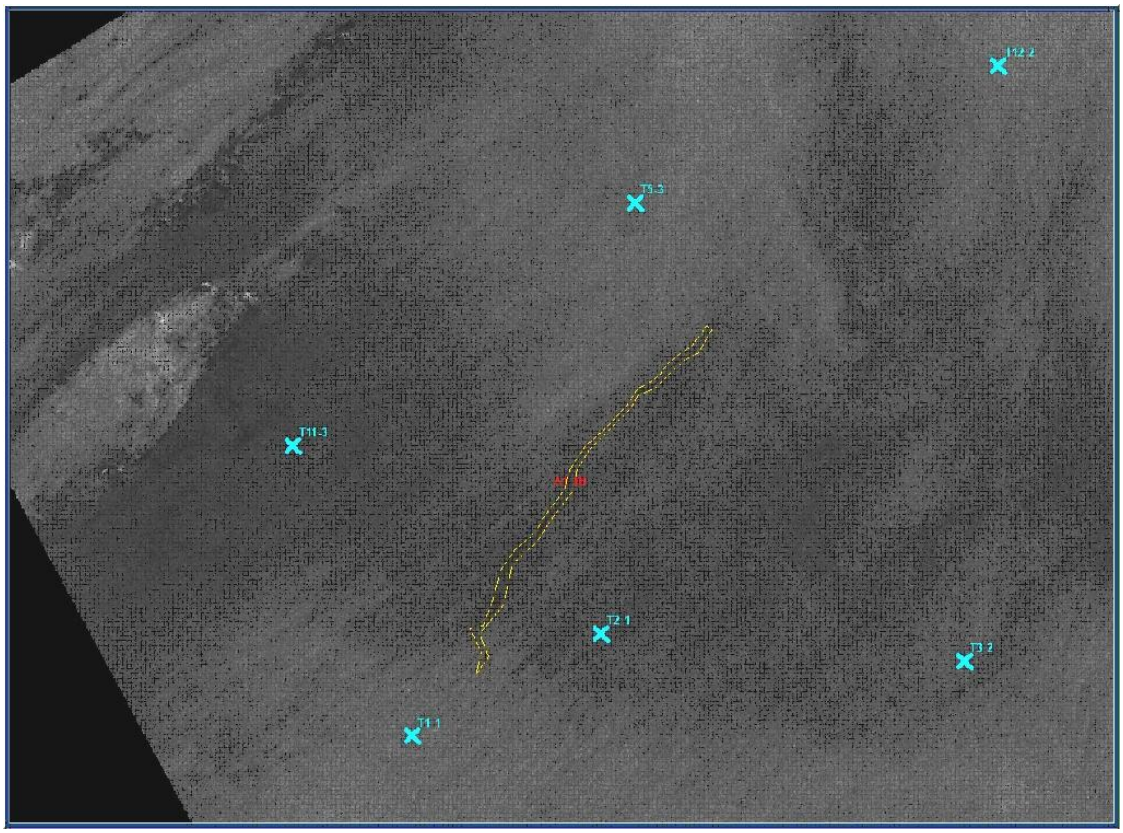

Figure 15. Example of ISTOP slick detection product – Newfoundland (source: https://www.ec.gc.ca/glaces-ice/default.asp?lang=En&n=C5EE0C9F-1)

Figure 16 shows a detection product generated under CleanSeaNet comprising and annotated satellite image (left) and corresponding GIS layers (right). The shape of the potential slick in the satellite image indicates the possible trailing of oily waste from a vessel. The vessel was subsequently identified using AIS data on the right side of the graphic.

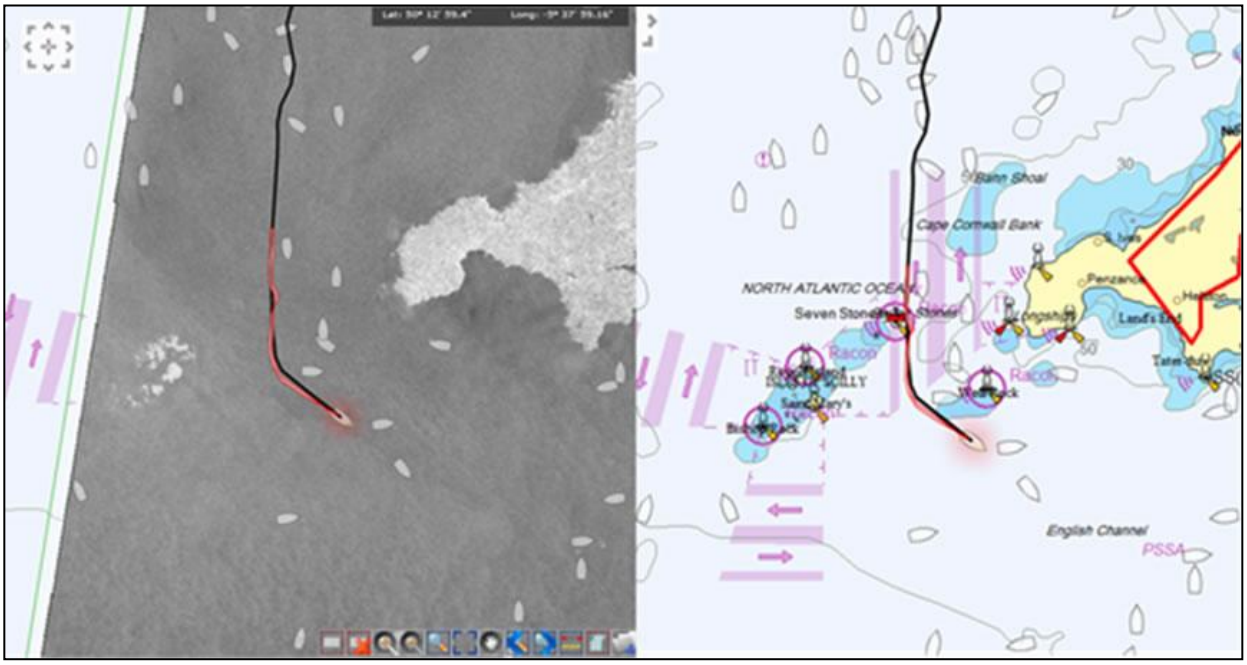


Figure 16. Example of CleanSeaNet slick detection product (source: http://www.emsa.europa.eu/csn-menu/csn-service/oil-spill-detection-examples/item/1873-oil-spill-detection-examples-maersk-kiera-february-2012.html)

PWS is a challenging area for oil slick detection due to its complex geographical and environmental conditions. Complex topography and coastline create wind shadow effects (diminished wind conditions) characterized by dark areas in the image as outline by the red rectangles in Figure 17. The wind on this date was generally from the North ranging from 1 to 8 $ms^{-1}$. Elongated dark streaks have also been observed in the images, which can be falsely identified as oil slicks. These could be caused by low wind areas or other oceanographic or environmental phenomena creating elongated low radar backscatter responses. The absence of ships in these areas is a further indication that the observed signatures are likely not caused by oil slicks.

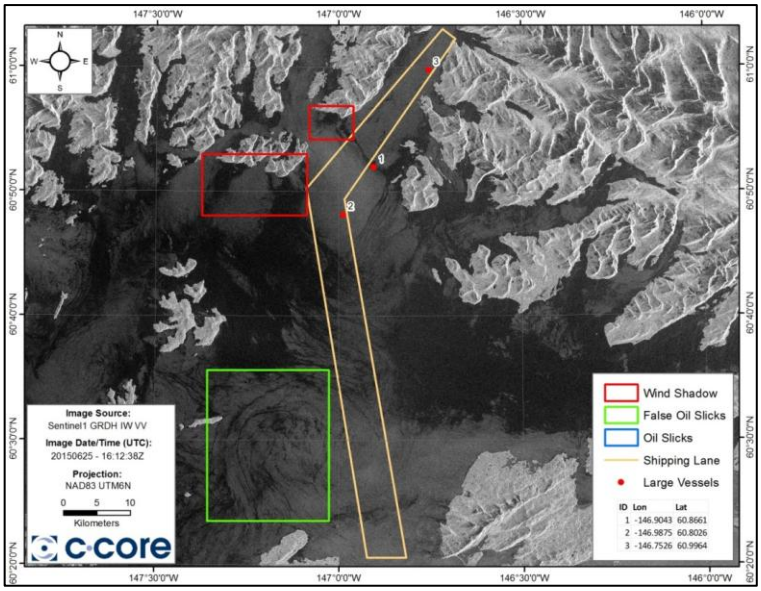


Figure 17. Image with wind shadow and oil slick look-alikes

In terms of vessel detection, small islands and rocks which can sometimes appear as bright targets and may pose challenges for correctly identifying such targets as vessels, particularly. Vessel targets can also be confused with icebergs, which can have similar radar signatures. However, the occurrence of false ship detections is minimized as analyst evaluate the physical radar response of a potential target together with applicable ancillary data (e.g. potential sources of icebergs, geospatial information layers depicting islands, pattern of freshwater inflow) during the QC process. A typical radar signature of a vessel, including high backscatter and prevalent side-lobing, is presented in Figure 18.

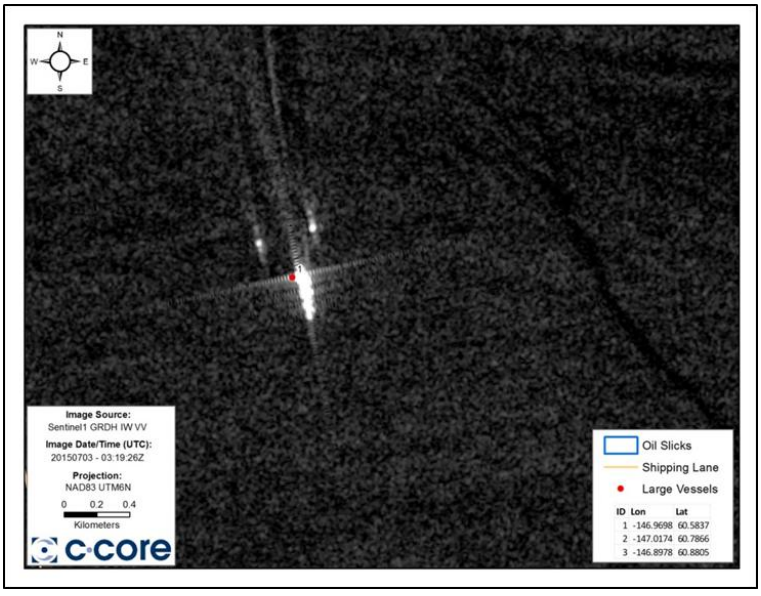


Figure 18. High backscatter and side-lobing characteristic for large vessels

# 6 RECOMMENDATIONS

Experiences from Europe and Canada demonstrate that satellite surveillance is effective at monitoring large areas for marine pollution incidents. Satellite-based monitoring has to be carried out with sufficient frequency on an ongoing basis. Due to their dynamic nature, the satellite monitoring of potential pollution events should be executed in near real-time, with information products available within two hours of image acquisition. Effective satellite-based monitoring requires the development and implementation of a streamlined operational process that integrates well with existing procedures on the user side (e.g. integration with other geospatial data, risk assessment, decision-making).

Freely available Senitinel-1 satellite radar imagery provides a unique opportunity to access operational radar imagery without incurring large data costs. The reliability of the new Sentinel-1 data availability, access and timeliness is expected to improve as the mission becomes fully operational. Extension of the AOI into the Gulf of Alaska is feasible, provided that suitable imagery is available. Sentinel-1 is currently being provided for the PWS AOI out to approximately 100 km into the Gulf of Alaska. Should Sentinel-1 imagery be required beyond this coverage, requests can be submitted to ESA via C-CORE to discuss the possibility of covering a larger area. Extending the area surveyed along major transportation corridors would increase the probability of early detection of accidental or illegal discharges from vessels.

Satellite radar imagery is very effective for iceberg and ship detection. In this investigation the capacity for vessel detection was limited to large vessels within the principal shipping lane. However, Sentinel-1 imagery can easily be analyzed to map all vessels within the AOI, and to discriminate between vessels and icebergs. Over time, this would allow the assessment of spatial and temporal distribution characteristics. As was demonstrated during this study, the same datasets and basic processing framework can be used for detecting vessels and oil slicks.

Although not addressed during this study, satellite monitoring can be extended to other phenomena of biological and economic significance, such as water quality, phytoplankton blooms, or sea ice. In the case of water quality and phytoplankton, optical imagery would be required to derive parameters of interest from water colour information. Free data sources of relevance in this context include the LANDSAT-8 and Sentinel-2 missions. In addition to being freely available, Sentinel-2 will provide a revisit frequency of several days, with a spatial resolution of up to 10 meters. Of course, the utility of optical imagery is limited by the occurrence of cloud cover.

The use of satellite SAR imagery for sea ice applications is well documented (Falkingham, 2014). If satellite monitoring is implemented for PWS on a routine basis, the focus could shift from pollution to ice monitoring during the winter, while taking advantage of a common basic processing framework.

Table 8 presents an overview of operational satellite missions suitable for marine environmental monitoring for the PWS area. Sentinel-1, Sentinle-2 and LANDSAT-8 data are available free of charge. COSMO-SkyMed, TerraSAR-X and Radarsat-2 are commercial missions, but discounts on data used for research purposes may be available.

Table 8. Selected satellite missions

| Mission | Configuration | Spatial Resolution [m] | Swath [km] | Revisit Frequency | Data Cost | Data Access |
|---|---|---|---|---|---|---|
| **COSMO-SkyMed** | • 4-satellite constellation<br>• X-Band SAR<br>• Single or dual-pol (HH, VV, HV, VH)<br><br>Tasking required; archive available; continuity mission planned | 1-100 | 10-200 | Daily | Commercial pricing | https://earth.esa.int/web/guest/data-access/catalogue-access |
| **Radarsat-2** | • C-Band SAR<br>• Single, dual or quad-pol (HH, VV, HV, VH)<br><br>Tasking required; archive available; continuity mission planned | 1-150m | 50-500 | 2-3 days | Commercial pricing | http://gs.mdacorporation.com/CustomerSupport/CustomerSupport.aspx |
| **TerraSAR-X** | • X-Band SAR<br>• Single or dual-pol (HH, VV, HV, VH)<br><br>Tasking required; archive available; continuity mission planned | 1-40 | 4-270 | 1-3 days | Commercial pricing | http://www.geo-airbusds.com/terrasar-x/ |
| **Sentinel-1** | • 2-satellite constellation<br>• C-Band SAR<br>• Single or dual-pol (HH, VV, HV, VH)<br><br>Sentinel-1A currently in orbit; Sentinel1B to be launched in 2016 | 5-40 | 20-400 | 1-3 days (Sentinel-1A and 1B) | Free | https://sentinel.esa.int/web/sentinel/sentinel-data-access. |
| **Sentinel-2** | • 2-satellite constellation<br>• 4 visible channels<br>• 6 NIR channels<br>• 3 SWIR channels<br><br>First satellite to be launched in 2015; systematic acquisition, no | 10-60 | 290 | <5days | Free | https://sentinel.esa.int/web/sentinel/user-guides/sentinel-2-msi;jsessionid=B965AAC9E156AC4A52BD25FAD4BB7A1C.eo |

| Mission | Configuration | Spatial Resolution [m] | Swath [km] | Revisit Frequency | Data Cost | Data Access |
|---|---|---|---|---|---|---|
| | tasking required; | | | | | disp-prod4040 |
| **LANDSAT 8** | • 1 Panchromatic channel<br>• 4 visible channels<br>• 1 NIR channel<br>• 3 SWIR channels<br>• 2 TIR channels<br><br>Provides continuity to earlier LANDSAT missions; systematic acquisition, no tasking required; archive available | 15 - 60 | 185 | 16 days | Free | http://landsat.gsfc.nasa.gov/?page_id=4071 |

The monitoring demonstration carried out during this investigation was too short to provide an adequate assessment of the occurrence of oil slicks in PWS. Going forward, the following actions are proposed to strengthen RCACs capacity for environmental monitoring and decision-making:

- Take advantage of freely available Sentinel-1 imagery over PWS to implement an ongoing, regular satellite surveillance program
- The monitoring should be carried out at a meaningful frequency (once fully operational, Sentinel-1 imagery should be available over PWS at least twice per week)
- Implement a capacity for image analysis in near real-time, together with suitable response actions to potential slicks detected (e.g. identify pollution control authorities)
- In addition to potential oil slicks, the satellite monitoring program should consider the detection of vessels and icebergs in the PWS area
- Over time, satellite-based products should be re-analyzed to reveal spatial and temporal distributions of potential oil slicks, vessels and icebergs
- The design of a satellite monitoring program should be flexible to accommodate future additions (e.g. water quality extracted from Sentinel-2 imagery)

# 7 REFERENCES

ASL (2012) Semi-Automated Classification of Oil slicks at sea using RADAR and Optical imagery (SACORO), PR-717.

Babiker, M.; Kloster, K.; Sandven, S. and Hall, R. (2010). "The Utilization of Satellite Images for the Oil in Ice Experiment in the Barents Sea", SINTEF Materials and Chemistry, SINTEF, Oil in Ice – JIP, Report No. 29.

Bogdanov, A. Robbe, N., Wald, L. and Cauneau, F (2005) Data Integration System for Marine Pollution and Water Quality. Final Report on Multi-Source Data fusion and Algorithms. DISMAR Report 16, 68 pp.

Brekke, C. and Solberg, A.H.S. (2005) Oil spill detection by satellite remote sensing. Remote Sensing of Environment, Vol. 95 (1), pp. 1-13.

Campbell, J. B. and Wynne, R. H. (2011) Introduction to Remote Sensing, 5th Edition (New York, The Guilford Press).

Environment Canada. (2015) Integrated Satellite Tracking of Pollution (ISTOP), retrieved from: https://www.ec.gc.ca/glaces-ice/default.asp?lang=En&n=40897129-1

European Maritime Safety Agency (EMSA) (2011) CleanSeaNet First Generation, 16 April 2007 - 31 January 2011, retrieved from: http://www.emsa.europa.eu/csn-menu/csn-how-it-works/items.html?cid=122&id=1309

EMSA (2015) CleanSeaNet Basic Training for Duty Officers – Alerting, Earth Observation Services Department C: Operations/C2.3, retrieved from: http://www.emsa.europa.eu/csn-menu/2015-04-15-07-09-03/training-material.html

European Space Agency (ESA) (2013) Sentinel-1 User Handbook (2013). GMES-S1OP-EOPG-TN-13-0001, retrieved from: https://sentinel.esa.int/documents/247904/685163/Sentinel-1_User_Handbook

ESA (2015) Sentinel High Level Operations Plan 2.0. COPE-S1OP-EOPG-PL-15-0020, retrieved from: https://sentinel.esa.int/documents/247904/685154/Sentinel_High_Level_Operations_Plan

Falkingham, J. (2014) Global Satellite Observation Requirements for Floating Ice Focusing on Synthetic Aperture Radar. Contract Report for Environment Canada , 78pp.

Ferraro, G., Baschek, B., de Montpellier, G., Njoten, O., Perkovic, and M., Vespe, M. (2010) On the SAR derived alert in the detection of oil spills according to the analysis of the EGEMP. Marine Pollution Bulletin 60 (2010) 91–102.

Fingas, M. F. and Brown, C. E. (1997) Review of Oil Spill Remote Sensing, Spill Science and Technology Bulletin, 4(4), pp. 199-208.

Gade, M.; Alpers, W.; Bao, M.; and Hühnerfuss, H. (1996) Measurements of the radar backscattering over different oceanic surface films during the SIR-C/X-SAR campaigns, Proceed. Intern. Geosci. Remote Sens. Sympos. (IGARSS)'96, IEEE, Piscataway, NJ, USA, 860-862.

Minchew, B.; Jones, C.E.; Holt, B. (2012) Polarimetric Analysis of Backscatter From the Deepwater Horizon Oil Spill Using L-Band Synthetic Aperture Radar. IEEE Transactions on Geoscience and Remote Sensing, vol.50, no.10, pp.3812-3830.

Solberg, A.H.S.; Storvik, G.; Solberg, R.; Volden, E. (1999) Automatic detection of oil spills in ERS SAR images. IEEE Transactions on Geoscience and Remote Sensing vol.37, no.4, pp.1916-1924.

Solberg, A. H. S.; Brekke, C. and Hursøy, P. O. (2007) Oil Spill Detection in Radarsat and Envisat SAR Images, IEEE Transactions on Geoscience and Remote Sensing, 45, 0196-2892.

Solberg, A.H.S. (2012) Remote Sensing of Ocean Oil-Spill Pollution. *Proceedings of the IEEE*, vol.100, no.10, pp.2931-2945.

Tarchi, D. (2005) Detecting and deterring illicit discharges. Satellite Monitoring and Assessment of Sea-based Oil Pollution, Istanbul, 13-14 June 2005

Topouzelis, K. N. (2008) Oil Spill Detection by SAR Images: Dark Formation Detection Feature Extraction and Classification Algorithms. Sensors, 8, pp. 6642 – 6659.

Van Zyl, J. and Kim, Y. (2011) Synthetic Aperture Radar Polarimetry (New Jersey, John Wiley & Sons).

**LAST PAGE OF DOCUMENT**